esa

ECOSPHERE

Allometric relationships for *Quercus gambelii* and *Robinia neomexicana* for biomass estimation following disturbance

Dan J. Krofcheck, Marcy E. Litvak, and Matthew D. Hurteau†

Department of Biology, University of New Mexico, Albuquerque, New Mexico, USA

Citation: Krofcheck, D. J., M. E. Litvak, and M. D. Hurteau. 2019. Allometric relationships for *Quercus gambelii* and *Robinia neomexicana* for biomass estimation following disturbance. Ecosphere 10(10):e02905. 10.1002/ecs2.2905

Abstract. In the southwestern USA, increases in size, frequency, and severity of wildfire are driving the conversion of forests to shrub-dominated ecosystems. Increases in drought extent and severity, coupled with the way that shrub-dominated systems are perpetuated by high-severity fire, predisposes these post-disturbance landscapes to remain in a non-forest condition. Consequently, understanding the distribution of aboveground biomass in post-disturbance, shrub-dominated ecosystems is central to constraining the uncertainty surrounding how these ecosystems interact with light and water to sequester carbon. Here we present allometric regressions for *Quercus gambelii* (Gambel oak) and *Robinia neomexicana* (New Mexico locust), two species that dominate post-fire landscapes in the southwestern USA. Our allometric regressions are designed to be driven by either field plot or high-resolution remote sensing data, using either shrub area or shrub volume to estimate biomass.

Key words: allometry; biomass; locust; oak; *Quercus gambelii;* remote sensing; *Robinia neomexicana;* wildfire.

Received 31 July 2019; accepted 3 September 2019. Corresponding Editor: Dawn M. Browning.

† **E-mail:** mhurteau@unm.edu

Introduction

Anthropogenic climatic change is increasing the rate and extent of uncharacteristic wildfire across the semi-arid southwestern USA (Dennison et al. 2014, Singleton et al. 2019). A legacy of fire exclusion has altered the structure of frequent-fire adapted forests characteristic of the region, increasing the likelihood of high-severity wildfire (Allen et al. 2002, Singleton et al. 2019). As more of the forested landscape experiences stand-replacing wildfires, landscape conversion from forest to shrub-dominated ecosystems is becoming more common (Parks et al. 2014, Coppoletta et al. 2016). Many shrub species re-sprout following fire, and following high-severity wildfire, shrubs can become the most abundant, if only woody vegetation, inside the perimeter of high-severity patches (Savage and Mast 2005, Coop et al. 2016, Guiterman et al. 2018), resulting in large and lasting changes to ecosystem structure and function.

The wildfire-catalyzed reallocation of carbon across the landscape from a vertically stratified coniferous forest canopy to short stature vegetation has significant and lasting implications for how vegetation across the landscape interacts with energy and water to sequester carbon (Amiro et al. 1999, Law et al. 2001, Bowman et al. 2009). Ecosystem light use is substantially reduced following these disturbances due to a combination of the large decrease in leaf area index (LAI) and transition to seasonal oscillation of LAI associated with deciduous plant phenology (Montes-Helu et al. 2009). Paired with the shorter growing season of deciduous vegetation compared to evergreen canopies, shifts in sensible heat fluxes trend toward a warmer landscape, due in part to lower per leaf area transpiration rates characteristic of shrub canopies (Fang et al.

2017). Together, these changes in how the vegetation interacts with light and water decrease both ecosystem productivity and the total stocks of above- and belowground carbon storage. Characterizing the distribution of carbon across post-disturbance landscapes is critical to understanding how a change in allocation of carbon will ultimately affect water ecosystem and energy balance (Gibbs et al. 2007).

As the abundance and extent of these post-disturbance ecosystems increases, so will the spatial challenges associated with characterizing carbon stocks. Conventional approaches to characterizing vegetation carbon stocks spatially make use of allometric relationships between size and shape of tree and shrub species to model the total biomass and carbon content of vegetation in both wood and foliar components (Jenkins et al. 2004, Chojnacky et al. 2013). Plot-based measurements of the stem, root collar, or diameter of the trunk at breast height are then leveraged to scale across larger extents, often with the use of remote sensing imagery from aerial or satellite data. Yet, the majority of the remote sensing data sets used to facilitate the scaling effort do not provide the same measurements as those that were used to generate the allometry and subsequently can produce mixed results (Lu 2006, Powell et al. 2010). For example, fractional cover or crown dimensions are used with moderate-to-high spatial resolution data, yet root collar diameter and height may have been used to develop the allometry (Krofcheck et al. 2016).

The increasing accessibility of high-resolution aerial and satellite remote sensing imagery, however, permits the scaling of allometric relationships that are built from direct crown area measurements across large extents (Asner et al. 2003, Gonzalez et al. 2010, Colgan et al. 2013). Including three-dimensional structural data (e.g., height and volume) in the allometric scaling effort further increases the capability to predict carbon stocks in short stature ecosystems, and can help mitigate some of the problems associated with using two-dimensional imagery to delineate individual shrubs in dense systems (Krofcheck et al. 2016). Developing relationships that relate shrub area and volume to biomass permits the application of remote sensing products to quantify the distribution of shrub biomass across spatial scales relevant to informing post-disturbance decision-making.

Here we present allometric scaling relationships for two of the most abundant shrub species in southwestern U.S. post-fire landscapes: *Quercus gambellii* (oak) and *Robinia neomexicana* (locust). Specifically, we sought to derive species-specific and grouped relationships to predict total biomass from shrub dimensions retrievable by both ground sampling and remote sensing applications. Further, we demonstrate the application of these allometric scaling relationships in a post-fire landscape using high-resolution remote sensing data collected via a small unmanned aerial system (sUAS).

Materials and Methods

Site description

We harvested shrubs in two 4 ha research sites in northern New Mexico, one in unburned ponderosa pine (*Pinus ponderosa*) forest and one within the perimeter of a high-severity fire patch that was ponderosa pine dominated prior to the fire, to develop our allometric equations. These research sites were selected because they represent the typical pre- and post- high-severity wildfire vegetation assemblages for semi-arid ponderosa pine forest in the southwestern USA. The unburned site is located in a ponderosa pine forest in the Valles Caldera National Preserve, and has been selected because it is shown to be a broad representative of southwestern ponderosa pine forest across the region (see Anderson-Teixeira et al. 2011, for a full site description). Our second site is located roughly 16 km SE, in the footprint of the Las Conchas fire that burned in 2011 on the east flank of the Jemez Mountains in northern New Mexico. The fire burned approximately 63,130 ha, 20% of which burned at high severity, and burned over five prior wildfire footprints. In forested areas that had not been impacted by prior wildfire, the Las Conchas burned at high severity. In areas where the Las Conchas fire burned over previous fires that had shifted the vegetation from forest to non-forest, the Las Conchas fire reinforced the vegetation change (Coop et al. 2016).

We sampled the unburned site at four locations within the 4 ha research area, each at 2500 m elevation, where the mean annual precipitation (MAP) is 550 mm and the mean annual temperature (MAT) is 9.8°C. We sampled the post-fire site at six locations along an elevation gradient ranging from 2400 to 2750 m, with a MAP of 482.14 mm and MAT of 8.34°C (DAYMET, Thornton et al. 2012). Soil type at the unburned site is a mixture of Cosey-Jarmillo association and Redondo, whereas the soil type at the post-fire sites is predominately a mixture of Lacueva and Bearsprings peak families (USDA Soil Data Explorer, https://websoilsurvey.sc.egov.usda.gov).

The understory of the unburned site is co-dominated by oak and herbaceous species. Locust was not captured in the sampling plots. The burned sites are co-dominated by oak and locust, with no conifer canopy cover and very few surviving trees. We selected Gambel oak and New Mexico locust because they co-occur with ponderosa pine and are common in patches burned by high-severity fire because they re-sprout following fire (Wagner et al. 1992, Muldavin et al. 2011, Kaufmann et al. 2016).

Sampling description and specific leaf area calculation

All destructive harvesting took place between June and August in 2017 and 2018, resulting in the harvest of 17 locust and 11 oak from the burned sites and 44 oak from the unburned site. We selected individual shrubs for harvest in an effort to capture the range and variability in height and area of individuals growing in both isolation and within clumps. We measured the height and two orthogonal crown diameters for each shrub, then cut the individual at the base, and placed each into large paper bags at the field site. We then dried the cut vegetation at 65°C for 3–7 d, or until the vegetation was fully dried as determined by successive weighing. We did not include any belowground material in our sampling. For a subset of six individuals of each species, we collected branches of average length and leaf number for each individual and separated the leaf material from the woody material. The leaf area of these samples was measured on a flatbed scanner before the foliar and woody materials were dried and the rest of the samples were also weighed following the same procedure (Fig. 1). The leaf scans were then aggregated and processed using ImageJ to calculate the specific leaf area (SLA) and total leaf area per unit dry weight (Schneider et al. 2012).

Allometry generation and error propagation

We used linear regression to predict shrub biomass using either shrub area or shrub volume for individual species and both species combined. We calculated the volume of an ellipsoid from the measured crown dimensions and used one-half of the ellipsoid to estimate shrub volume. We estimated shrub area by using the two orthogonal crown diameters to calculate the area of an ellipse. We used root mean-squared error, adjusted R^2, and leave-one-out cross-validation to assess model fit. We tested for significance between sample populations using univariate t tests. We incorporated the salient sources of model error in our regressions, including the measurement uncertainty made in the field (±5 cm per measurement) and biomass measurements made in the lab (±0.01 g per bag). We propagated that uncertainty through to each observation using a Monte-Carlo approach to

Fig. 1. Leaf scan composite of leaf samples from *Quercus gambelii* (left) and *Robinia neomexicana* (right) exhibiting morphology typical for the species in northern New Mexico.

bootstrapping the linear regression. We ran 1000 iterations of the curve fitting process wherein for each iteration and input variables, we multiplied a random draw from a normal distribution (mu = 0, sigma = 0.5) with the corresponding propagated uncertainty (Asner et al. 2003, Gonzalez et al. 2010, Krofcheck et al. 2016). Assessments of significant statistical relationships were determined by a P-value <0.05. All statistical tests, model fitting, and figure generation were performed in Python 3.6 (Python Software Foundation, Wilmington, Delaware, USA).

Small footprint biomass determination using a small unmanned aerial system

We used a sUAS hexacopter to collect imagery in a 6.7-ha site located in the Las Conchas fire perimeter. Images were collected in July 2018 using a custom-built hexacopter carrying a Sony a6000 camera (Sony Corporation, Tokyo, Japan) with a 19 mm prime lens, capturing imagery in the RAW format. We integrated the camera with an EMLID Reach global navigation satellite system (GNSS) receiver on the sUAS such that the camera shutter activation would be recorded as an event by the EMLID Reach (www.emlid.com). A second EMLID Reach GNSS receiver was positioned as a base station running concurrently during the sUAS operation. We conducted flight planning in Mission Planner (v1.3), with all flights occurring within visual line of sight and at 80 m above ground level, resulting in a ground sample distance of 1.4 cm per pixel. We designated a front and side image overlap of 85% and 80%, respectively, with a total of 80 images collected. The precise location of each image photo-center was determined using a post-processed kinematic workflow in RTKLib (v2.4.3, http://www.rtklib.com/). The RAW format images were converted to 16-bit linear TIFF files in Python 3.6, and imported into Agisoft Metashape for structure from motion (SfM) processing. We followed a procedure similar to Cunliffe et al. (2016) to convert the imagery to a raster of canopy heights and an orthomosaic. We conducted inverse watershed segmentation on the canopy height model to extract the shrub crowns as individual objects. We only included objects >0.3 and <5 m in height for this example analysis. Finally, we vectorized the resulting objects into an ESRI shapefile and calculated the area and volume of each canopy object, storing them as attributes of the shapefile. This workflow allowed us to apply area- or volume-based allometric relationships to each canopy object in our analysis extent along with the error propagation results, similar to Krofcheck et al. (2016).

Results

The distributions of crown area and crown volume for the individuals we harvested are shown in Fig. 2. The majority of oaks sampled at the unburned site had smaller areas and volumes because they were growing under an intact ponderosa pine canopy. The lack of tree canopy at the burned site and its influence on light and water availability resulted in a wider distribution of oak sizes, with volumes ranging from 1.3 e^{-4} to 0.33 m^3 at the unburned site and 0.10 to 11.57 m^3 at the burned site.

Log normalization of area and volume as linear model predictors of dry biomass improved adjusted R^2 values over the untransformed relationship and explained 91–97% of the variability in the natural log of dry biomass (Fig. 3, Table 1). Given the improved adjusted R^2 and decreased root mean square error (RMSE) of the log-normalized fits, we propagated the uncertainty in the dimensional and biomass measurements accordingly and bootstrapped the regressions to develop a mean and variance of the fit statistics (Table 1).

The oak leaves were gently lobed with median line symmetry and were slightly smaller than the pinnately compound leaves of the locust (Fig. 1). The SLA of oak ($0.01 \pm 9.7\ e^{-4}$) was significantly higher than that of the locust ($0.009 \pm 8.5\ e^{-4}$, $P < 0.05$; Fig. 4).

When we applied the resulting combined species and volume-based allometry to our demo sUAS analysis extent, we calculated 0.75 ± 0.05 Mg of biomass/ha (Fig. 5).

Discussion

The semi-arid forests of the southwestern USA have historically been shaped and maintained by wildfire, yet fire exclusion and climatic change are altering the way wildfire interacts with forests across the region. As high-severity, stand-replacing wildfire increases in the southwestern USA, post-fire communities dominated by shrubs are becoming increasingly common. Since

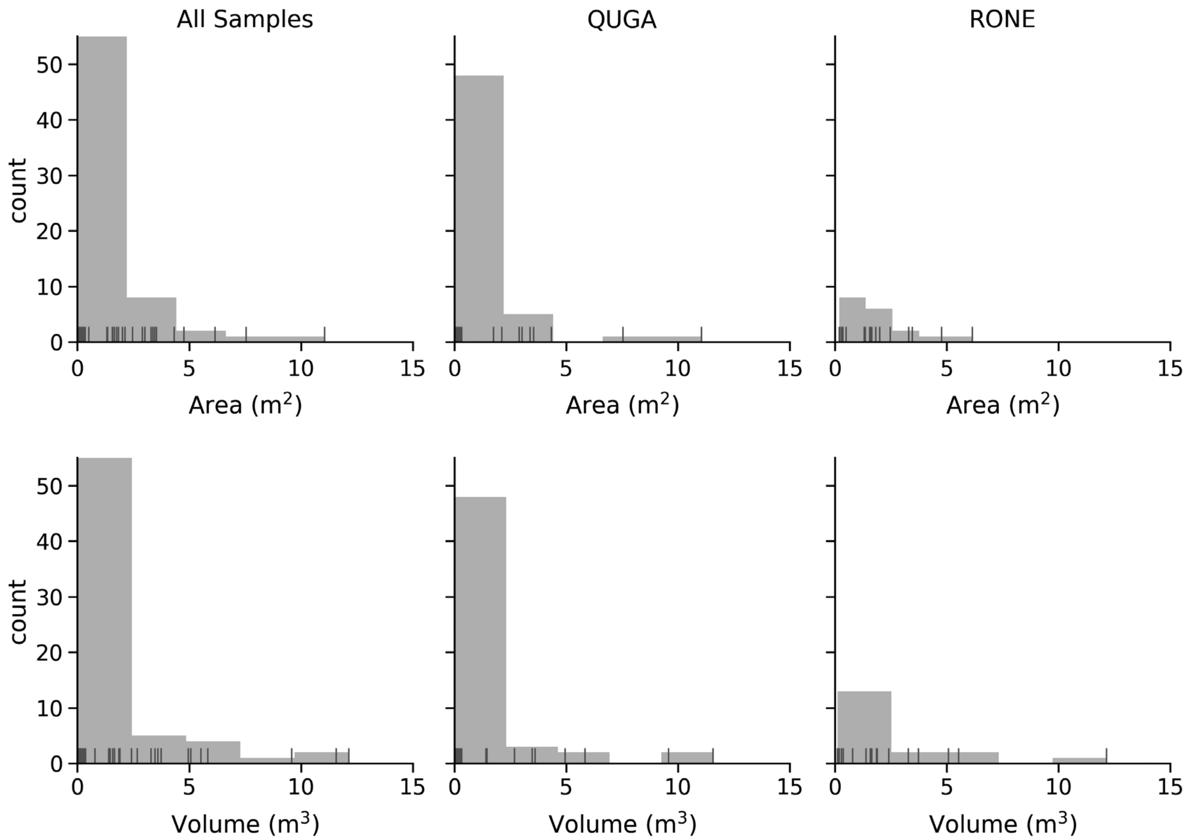

Fig. 2. Distributions for *Quercus gambelii* (QUGA) and *Robinia neomexicana* (RONE) area (top) and volume (bottom) measurements that informed the individual and combined allometries. The *x*-axis tick marks denote the area and volume of samples within each bin.

both of these shrub species re-sprout following fire, the near-term post-fire structural transformation from forest to a low-statured shrub canopy and standing dead trees increases the likelihood that these severely burned patches experience another high-severity fire if they re-burn (Coppoletta et al. 2016, Walker et al. 2018). Further, long distances to mature surviving pines paired with changes to the light and soil moisture environment following severe wildfire can be an impediment to conifer regeneration (Chambers et al. 2016).

The combination of increased likelihood of subsequent high-severity fire and decreased conifer regeneration in these systems has the potential to convert landscapes that were once forests to a significantly less productive state dominated by shrubs (Coop et al. 2016, Guiterman et al. 2018). The cascading implications for the fate of carbon, water, and energy balance at regional scales from vegetation type change make it critical that we develop the means to characterize both how these post-disturbance landscapes are structured and what the implications of that structure are in terms of ecosystem function both spatially and temporally.

Our allometric relationships can be used to estimate the biomass of individual shrub canopies in unburned and post-fire landscapes in the southwestern USA where oak and locust cover is not contiguous. Further, because we include both area and volume equations and their associated uncertainties, shrub biomass can be spatially scaled following conventional plot- and area-based approaches paired with estimates of percent cover across larger areas.

However, we developed these allometries with the intent to aid characterizing shrub

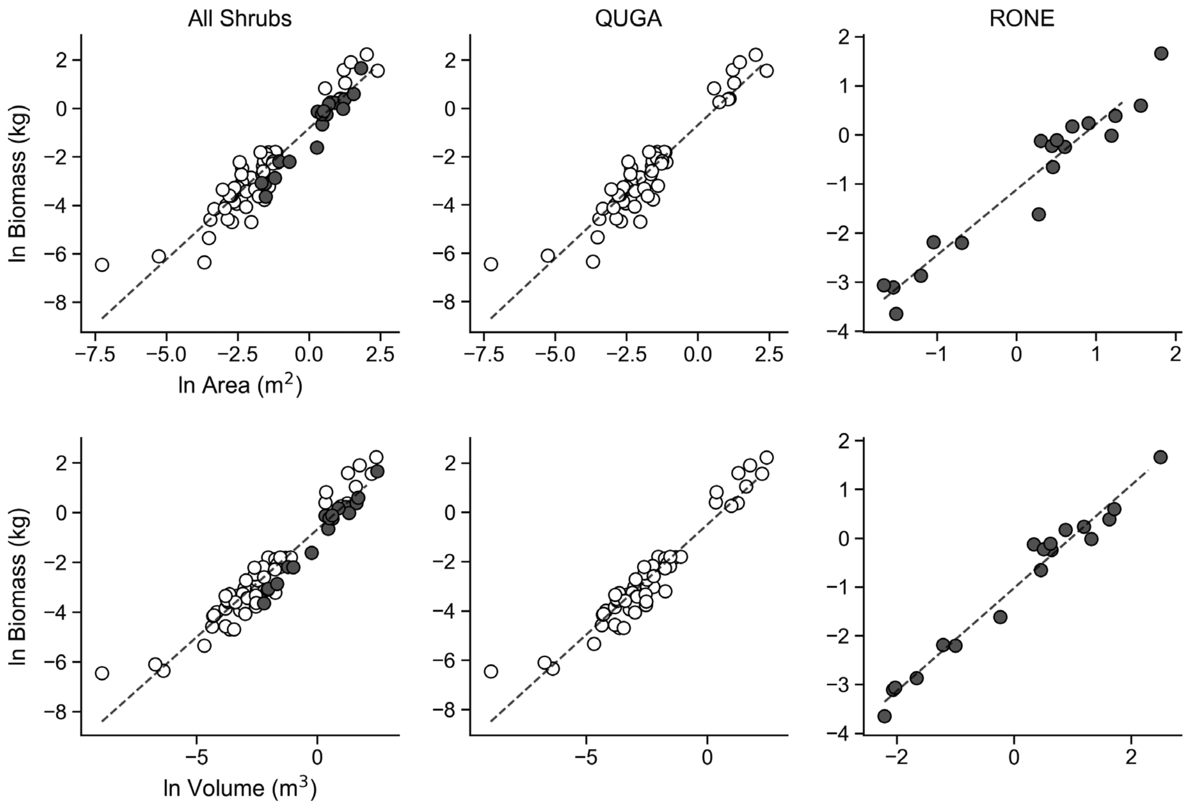

Fig. 3. Linear regression relating log-normalized field measured crown area (top) and volume (bottom) to log-normalized dried biomass for *Quercus gambelii* (QUGA), *Robinia neomexicana* (RONE), and both species combined. Fit statistics are reported in Table 1.

Table 1. Regression fit statistics for the area (top)- and volume (bottom)-based shrub allometries for the model form $y = m \cdot x + \beta$, where y is the natural log of biomass and x is either the natural log of shrub area or volume.

Variable	m	β	RMSE (kg)	Adjusted R^2	$m\sigma$	$\beta\sigma$
Crown area allometry						
Oak	1.119	−0.679	2.01	0.874	0.064	0.087
Locust	1.331	−1.115	1.6	0.933	0.022	0.019
Combined	1.091	−0.813	1.95	0.888	0.048	0.042
Crown volume Allometry						
Oak	0.898	−0.5	1.77	0.915	0.037	0.068
Locust	1.054	−1.026	1.23	0.97	0.008	0.009
Combined	0.866	−0.683	1.76	0.919	0.026	0.032

Note: Mean values are reported for the species-specific and combined regression statistics for both slope (m) and intercept (β), as well as the standard deviations resulting from 1000 replicate fits incorporating measurement uncertainty.

biomass across spatial extents relevant to the scale of high-severity wildfire patch size by making use of high-resolution remote sensing data and small unmanned aerial system (sUAS) surveys.

Remote sensing techniques capable of resolving individuals or clumps of shrubs, such as high-resolution satellite imagery (e.g., Worldview sensors), aerial surveys (e.g., NAIP), or sUAS acquisitions, can be paired with these allometric relationships to estimate the biomass across the landscape. In our example, we used sUAS imagery and SfM to construct three-dimensional models of the post-fire shrub canopy and estimated shrub biomass using the combined species volume–biomass relationship (Fig. 5). Here, the 6.7 ha analysis region contained 5.0 ± 0.23 Mg of shrub biomass (0.75 ± 0.05 Mg biomass/ha). This is a substantial reduction in biomass compared to our unburned site (141.3 Mg C ± 44.3 Mg biomass/ha; Remy et al. 2019).

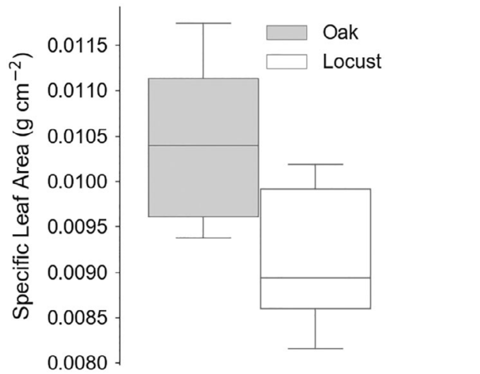

Fig. 4. Distribution of the specific leaf area of both oak (*Quercus gambelii*) and locust (*Robinia neomexicana*), $N = 6$ for both species.

The spatially continuous characterization of total vegetation biomass in a post-disturbance landscape is a powerful state variable that is required to understand ecophysiological processes and can be useful for informing post-fire management. Changes in biomass allocation over time, or aboveground productivity, are initially governed by, and ultimately affect, patterns of water and energy flux across the landscape. Consequently, the ability to characterize the spatial and temporal patterns in biomass change is central to understanding the development of

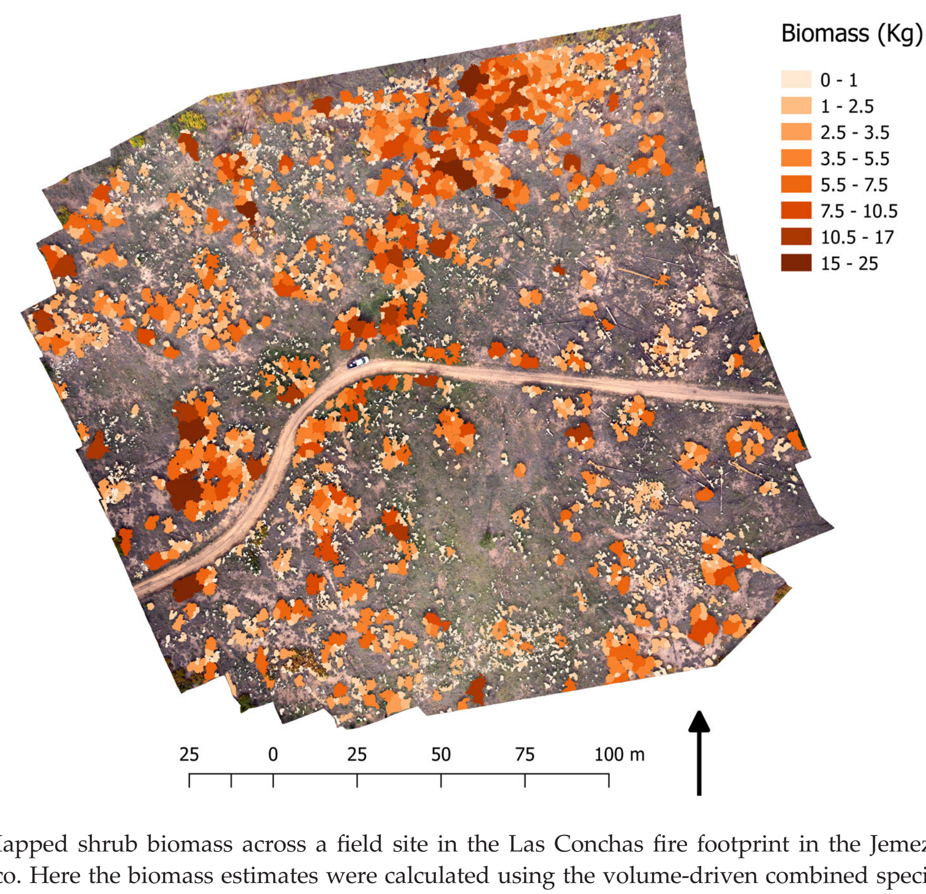

Fig. 5. Mapped shrub biomass across a field site in the Las Conchas fire footprint in the Jemez Mountains, New Mexico. Here the biomass estimates were calculated using the volume-driven combined species allometry, where only objects >0.3 and <5 m were considered in the analysis.

these ecosystems and the ecology they support. Changes in biomass allocation over time and across space also influence the way that a subsequent fire will interact with the landscape (Coop et al. 2016, Coppoletta et al. 2016). This approach can be used to quantify the post-fire ecosystem structure and inform fire spread modeling. Given the lack of information regarding the successional fate of these post-fire systems under changing climatic conditions and disturbance regimes, basic information regarding state variables like vegetation biomass will help to constrain uncertainty and improve estimates of landscape processes under contemporary and projected climates.

Acknowledgments

This work is supported by the Interagency Carbon Cycle Science program (grant no. 2017-67004-26486/project accession no. 1012226) from the USDA National Institute of Food and Agriculture, the Joint Fire Science Program under Project JFSP 16-1-05-8, the National Science Foundation grant EAR-1331408 in support of the Catalina-Jemez Critical Zone, and the Department of Energy Ameriflux Management Project subcontract no. 7074628. We acknowledge the work of field technicians including Melissa Baciagalupa, Joeseph Crockett, and Kevin Willson for the collection and preparation of the biomass material used in this analysis.

Literature Cited

Allen, C. D., M. Savage, D. A. Falk, K. F. Suckling, W. Thomas, T. Schulke, P. B. Stacey, P. Morgan, M. Hoffman, and J. T. Klingel. 2002. Ecological restoration of southwestern ponderosa pine ecosystems: a broad perspective. Ecological Applications 12:1418–1433.

Amiro, B. D., J. I. MacPherson, and R. L. Desjardins. 1999. BOREAS flight measurements of forest-fire effects on carbon dioxide and energy fluxes. Agricultural and Forest Meteorology 96:199–208.

Anderson-Teixeira, K. J., J. P. Delong, A. M. Fox, D. A. Brese, and M. E. Litvak. 2011. Differential responses of production and respiration to temperature and moisture drive the carbon balance across a climatic gradient in New Mexico. Global Change Biology 17:410–424.

Asner, G. P., S. Archer, R. F. Hughes, R. J. Ansley, and C. A. Wessman. 2003. Net changes in regional woody vegetation cover and carbon storage in Texas Drylands, 1937–1999. Global Change Biology 9:316–335.

Bowman, D. M. J. S., et al. 2009. Fire in the Earth system. Science 324:481–484.

Chambers, M. E., P. J. Fornwalt, S. L. Malone, and M. A. Battaglia. 2016. Patterns of conifer regeneration following high severity wildfire in ponderosa pine – dominated forests of the Colorado Front Range. Forest Ecology and Management 378:57–67.

Chojnacky, D. C., L. S. Heath, and J. C. Jenkins. 2013. Updated generalized biomass equations for North American tree species. Forestry 87:129–151.

Colgan, M. S., G. P. Asner, and T. Swemmer. 2013. Harvesting tree biomass at the stand level to assess the accuracy of field and airborne biomass estimation in savannas. Ecological Applications 23:1170–1184.

Coop, J. D., S. A. Parks, S. R. McClernan, and L. M. Holsinger. 2016. Influences of prior wildfires on vegetation response to subsequent fire in a reburned Southwestern landscape. Ecological Applications 26:346–354.

Coppoletta, M., K. E. Merriam, and B. M. Collins. 2016. Post-fire vegetation and fuel development influences fire severity patterns in reburns. Ecological Applications 26:686–699.

Cunliffe, A. M., R. E. Brazier, and K. Anderson. 2016. Ultra-fine grain landscape-scale quantification of dryland vegetation structure with drone-acquired structure-from-motion photogrammetry. Remote Sensing of Environment 183:129–143.

Dennison, P. E., S. C. Brewer, J. D. Arnold, and M. A. Moritz. 2014. Large wildfire trends in the western United States, 1984–2011. Geophysical Research Letters 41:2928–2933.

Fang, W., N. Lu, Y. Zhang, L. Jiao, and B. Fu. 2017. Responses of nighttime sap flow to atmospheric and soil dryness and its potential roles for shrubs on the Loess Plateau of China. Journal of Plant Ecology 11:717–729.

Gibbs, H. K., S. Brown, J. O. Niles, and J. A. Foley. 2007. Monitoring and estimating tropical forest carbon stocks: making REDD a reality. Environmental Research Letters 2:45023.

Gonzalez, P., G. P. Asner, J. J. Battles, M. A. Lefsky, K. M. Waring, and M. Palace. 2010. Forest carbon densities and uncertainties from Lidar, QuickBird, and field measurements in California. Remote Sensing of Environment 114:1561–1575.

Guiterman, C. H., E. Q. Margolis, C. D. Allen, D. A. Falk, and T. W. Swetnam. 2018. Long-term persistence and fire resilience of oak shrubfields in dry conifer forests of northern New Mexico. Ecosystems 21:943–959.

Jenkins, J., D. Chojnacky, L. Heath, and R. Birdsey. 2004. Comprehensive database of diameter-based biomass regressions for North American tree species. General Technical Report NE-319. USDA Forest Service, Newtown Square, Pennsylvania, USA.

Kaufmann, M. R., D. W. Huisjen, S. Kitchen, M. Babler, S. R. Abella, T. S. Gardiner, D. McAvoy, J. Howie, and D. H. Page. 2016. Gambel oak ecology and management in the southern Rockies: the status of our knowledge. SRFSN Publication 2016-1. Colorado State University, Southern Rockies Fire Sciences Network, Fort Collins, Colorado, USA.

Krofcheck, D. J., M. E. Litvak, C. D. Lippitt, and A. Neuenschwander. 2016. Woody biomass estimation in a southwestern U.S. Juniper Savanna using LiDAR-derived clumped tree segmentation and existing allometries. Remote Sensing 8:453.

Law, B. E., P. E. Thornton, J. Irvine, P. M. Anthoni, and S. Van Tuyl. 2001. Carbon storage and fluxes in ponderosa pine forests at different developmental stages. Global Change Biology 7:755–777.

Lu, D. 2006. The potential and challenge of remote sensing-based biomass estimation. International Journal of Remote Sensing 27:1297–1328.

Montes-Helu, M. C., T. Kolb, S. Dore, B. Sullivan, S. C. Hart, G. Koch, and B. A. Hungate. 2009. Persistent effects of fire-induced vegetation change on energy partitioning and evapotranspiration in ponderosa pine forests. Agricultural and Forest Meteorology 149:491–500.

Muldavin, E., A. Kennedy, C. Jackson, P. Neville, T. Neville, K. Schultz, and M. Reid. 2011. Vegetation classification and map: Bandelier National Monument. Natural Resource Technical Report NPS/SCPN/NRTR—2011/438. National Park Service, Fort Collins, Colorado, USA.

Parks, S. A., C. Miller, C. R. Nelson, and Z. A. Holden. 2014. Previous fires moderate burn severity of subsequent wildland fires in two large western US wilderness areas. Ecosystems 17:29–42.

Powell, S. L., W. B. Cohen, S. P. Healey, R. E. Kennedy, G. G. Moisen, K. B. Pierce, and J. L. Ohmann. 2010. Quantification of live aboveground forest biomass dynamics with Landsat time-series and field inventory data: a comparison of empirical modeling approaches. Remote Sensing of Environment 114:1053–1068.

Remy, C. C., D. J. Krofcheck, A. R. Keyser, M. E. Litvak, S. L. Collins, and M. D. Hurteau. 2019. Integrating species-specific information in models improves regional projections under climate change. Geophysical Research Letters 46:6554–6562.

Savage, M., and J. N. Mast. 2005. How resilient are southwestern ponderosa pine forests after crown fires? Canadian Journal of Forest Research 35:967–977.

Schneider, C. A., W. S. Rasband, and K. W. Eliceiri. 2012. NIH Image to ImageJ: 25 years of image analysis. Nature Methods 9:671–675.

Singleton, M. P., A. E. Thode, A. J. S. Meador, and J. M. Iniguez. 2019. Increasing trends in high-severity fire in the southwestern USA from 1984 to 2015. Forest Ecology and Management 433:709–719.

Thornton, P. E., M. M. Thornton, B. W. Mayer, N. Wilhelmi, Y. Wei, R. Devarakonda, and R. B. Cook. 2012. Daymet: daily surface weather data on a 1-km grid for North America, version 2. ORNL DAAC, Oak Ridge, Tennessee, USA. http://dx.doi.org/10.3334/ORNLDAAC/1219

Wagner, M. R., R. E. Larson, and T. P. Craig. 1992. Ecology and silvics of New Mexico locust, *Robinia neomexicana*, with an emphasis on the arboreal form. Pages 53–57 *in* J. Hanover, K. Miller, and S. Plesko, editors. Proceedings: International Conference on Black Locust: Biology, Culture, and Utilization, East Lansing, Michigan, 17–21 June 1991. Michigan State University, East Lansing, Michigan, USA.

Walker, R. B., J. D. Coop, S. A. Parks, and L. Trader. 2018. Fire regimes approaching historic norms reduce wildfire-facilitated conversion from forest to non-forest. Ecosphere 9:e02182.

Data Availability

Data and code used in this study are available at https://digitalrepository.unm.edu/bio_data/4/